Non-rigid Elastic Registration of Retinal Images using Local Window Mutual Information

Philip A. Legg[a*], Paul L. Rosin[a†], David Marshall[a‡] and James E. Morgan[b§]

[a]School of Computer Science, Cardiff University. [b]School of Optometry, Cardiff University.

Abstract. In this paper we consider the problem of non-rigid retinal image registration between colour fundus photographs and Scanning Laser Ophthalmoscope (SLO) images. Registration would allow for cross-comparison between modalities, giving both appearence and reflectivity information which would provide clearer visualisation for demarcation of the optic nerve head as part of early glaucoma detection. Due to the differences in acquisition technique, along with alterations in the eye between acquisitions, there can be subtle non-rigid deformations present in the images that become apparent when performing rigid registration. Whilst this is negligible towards the centre of the SLO, the effect becomes much more noticable towards the periphery of the image, where it can be seen that not all blood vessels are aligned correctly. We propose a two-stage registration consisting of finding an initial rigid registration using Feature Neighbourhood Mutual Information [1], and then to use Local Window Mutual Information to quickly determine deformation parameters for a non-rigid solution. We test our method on 135 image pairs, with results showing improved registration accuracy compared to rigid registration.

1 Introduction

Image registration has become extensively popular within the medical community as a powerful diagnosis tool. Registration of two (or more) images into the same spatial alignment can be used to gain substantial information regarding a patient that simply cannot be provided by a single image. Registration tasks may involve inter-modal registration (e.g. generating retinal fundus maps [2]), or registering images taken over a period of time as a monitoring procedure. Recently, multi-modal registration has been widely adopted since the fusion of different modalities can offer much greater diagnostic information when analysing structural components, due to their different representations in the images, for example, registering Magnetic Resonance (MR) images with Computed Tomography (CT) images.

Mutual Information (MI) is a widely recognised approach suitable for registering images captured from different modalities. Simultaneously proposed by Viola [3] and Collignon [4], MI makes a statistical comparison between the images rather than an individual intensity comparison, making it a suitable similarity measure for multi-modal images. Given two images A and B, Mutual Information can be defined as $I(A;B) = H(A) + H(B) - H(A,B)$, where $H(A)$ is the entropy of image A, $H(B)$ is the entropy of image B and $H(A,B)$ is the joint entropy of both A and B. To register two images, we wish to find the spatial transformation that maximises $I(A;B)$. If we consider entropy as the dispersion of intensity values, then we wish to find where both A and B have many different intensities (e.g. anotomical structure) yet also where there is little dispersion (or rather, closer grouping) in the joint distribution (A,B). Studholme extended the standard algorithm to Normalized Mutual Information (NMI) [5], to account for varying number of samples in the distribution, given as $I(A;B) = \frac{H(A)+H(B)}{H(A,B)}$.

The image modalities to be registered are colour fundus photographs and Scanning Laser Ophthalmoscope (SLO) images. The fundus image gives very high quality appearance information whilst the SLO gives reflectivity and surface topography for the optic nerve head and retina. The fundus image clearly shows the boundary of the optic nerve head, whereas this is much more difficult to accurately mark on the SLO image. Registration of these images would allow for improved demarcation of the optic nerve head in both modalities as part of the monitoring stage for early detection of glaucoma disease. Comparing registered images over time would provide much clearer indication to the clinician of any changes that are occuring in the eye, and so suitable action could be taken.

Rueckert uses b-splines for performing non-rigid registration of mammographic images [6], whilst Rohr *et al.* uses Thin-Plate Splines [7] to register MR images using landmark data points. Unlike with MR/CT imaging, there is no clearly defined boundary (e.g. a human skull) that could aid as a landmark for registration between our two modalities. While a rigid transformation can successfully register some of our image pairs, Kubecka and Jan [8] recommend that the registration of fundus and SLO images should be generalized to elastic registration as there can be some degree

*E-mail: P.A.Legg@cs.cardiff.ac.uk
†E-mail: Paul.Rosin@cs.cardiff.ac.uk
‡E-mail: Dave.Marshall@cs.cardiff.ac.uk
§E-mail: morganje3@cardiff.ac.uk

of deformation between the two images, although they do not demonstrate doing this. Since the two images are not captured at the same time, any subtle changes in the eye such as movement or shape can affect whether a rigid or non-rigid transformation is required.

In this paper, we propose fully automated non-rigid registration of retinal images. Firstly, we perform Feature Neighbourhood Mutual Information (FNMI) [1] to find an initial rigid registration between the fundus image and the SLO image. We then use Local Window Mutual Information (LWMI) to refine the registration for each individual segment of the image. The refined registration is used to guide elastic deformation using a Thin-Plate Spline warp. The paper is organised as follows: Section 2 describes using FNMI to find the initial rigid registration. Section 3 gives details of extending this to a non-rigid registration. Section 4 shows our testing strategy and presents the results obtained compared to our original rigid registration. Finally, Section 5 gives some discussion of our proposed method.

2 Feature Neighbourhood MI

The first stage of our registration is to find an initial rigid registration that gives an initial alignment between the SLO image and the fundus image. We use FNMI to find the rigid transformation since it provides a high degree of accuracy for the modalities in question. FNMI incorporates multi-scale structural information from the images, along with spatial neighbourhood information. We found that this method gives a smooth surface function that tends to lead to a global maximum at the correct registration.

To perform FNMI registration, we use the original images along with the first derivative taken at scale $\sigma = 2$ pixels and $\sigma = 4$ pixels. Through investigation we found that using these two feature images gave high accuracy for our registration problem. We move our floating (SLO) image over our reference (fundus) image to find the position that returns the maximum value for FNMI. At each position, we create a feature vector for each pixel being registered consisting of 54 values; the pixel and its 8 surrounding neighbours from the floating image and its two feature images, and likewise for the overlapped region in the reference image. If our floating image consists of $m \times n$ pixels, then the complete feature matrix would be $P = 54 \times (m \times n)$.

Given matrix P, we normalize this by the mean and find the co-variance matrix given by $C = \frac{1}{N} PP^T$. FNMI is calculated by $H(C_A) + H(C_B) - H(C)$ where $H(C_A)$ is the entropy of the top-left quarter of C, $H(C_B)$ is the entropy of the bottom-right quarter of C and $H(C)$ is the entropy of C.

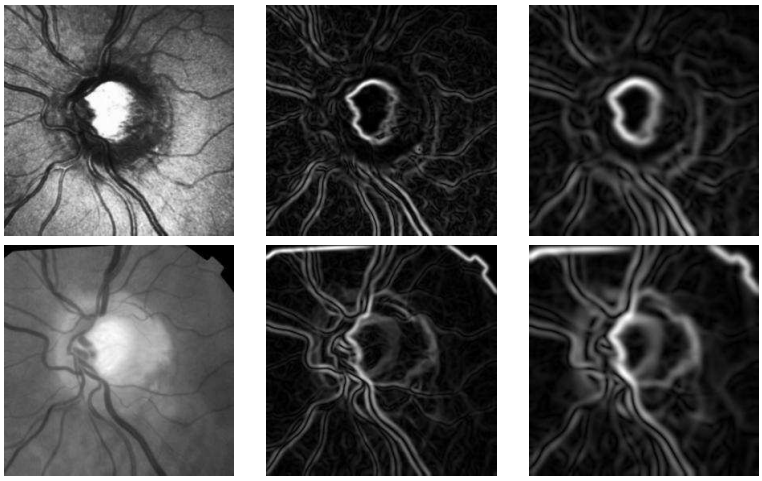

Figure 1. Top: SLO image with multi-scale gradient images ($\sigma = 2$ and 4). Bottom: Extract from fundus photograph with multi-scale gradient images ($\sigma = 2$ and 4).

To find our initial registration, we only consider rigid transformation (rotation and translation). We use the Nelder-Mead simplex search algorithm [9] to optimise our translation search; this is initially optimised over a set of rotations between the range $\pm 3^\circ$ with a step size of 0.5°. We also incorporate a 3-level image pyramid (full size, $\frac{1}{2}$ size and $\frac{1}{4}$ size) to search on a coarse-to-fine basis. At the coarse level we can search all rotations very quickly and find an initial estimate for the next level down. As we traverse down the pyramid, the rotation search range is restricted to $\pm 1^\circ$ to narrow the search range, which is fixed at the lowest level of the pyramid (full resolution).

3 Local Window Mutual Information

Using FNMI, we obtain a rigid registration between our two images that gives a good initial registration. Figure 2 shows the registration result which appears accurate; however while most of the blood vessels appear matched at the borders of the SLO image, there are some misalignments that can be noticed (highlighted in this example). This shows a typical example where the majority of the image appears fine, yet there is some subtle misalignment present, indicating that a non-rigid registration is required. We wish to correct this by performing Local Window Mutual Information (LWMI). This method aims to improve registration locally by considering individual windows within the image and shifting these within a constrained region based on the original image.

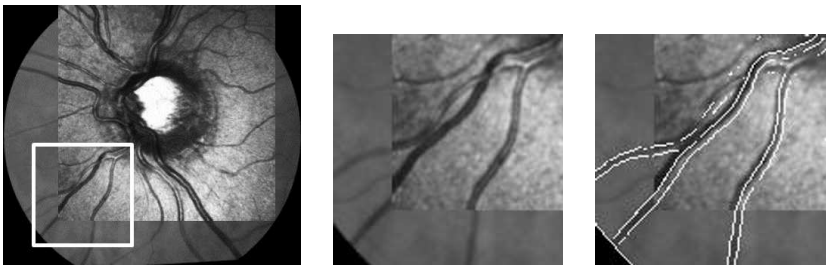

Figure 2. Left-to-right: Rigid Registration using FNMI, Close-up of misalignment, Close-up of misalignment showing correct edges from fundus.

Given the SLO image and its corresponding region from the fundus image (as found in Section 2), we subdivide the SLO image up into a set of 4×4 windows, with corresponding windows in the fundus image. The centre-points from these 16 windows define our initial control points for performing non-rigid deformation. For each of these windows, we further subdivide the image into another set of 4×4 windows, and compute NMI on each of these smaller windows. The LWMI is given by the sum of each of these smaller windows. We found that computing NMI on smaller regions in this fashion gave better accuracy than using larger regions such as the original 16 windows or the entire image. NMI is maximised where a 1-to-1 correspondence between intensities occurs. Therefore by adopting this local approach there is less influence from global lighting artefacts that can hinder the Mutual Information algorithm. Since LWMI makes many local comparisons it incorporates spatial consideration for each region within the image whilst having a runtime similar to traditional Mutual Information.

The range of translation shift that we search for is based on the observed deformations that occurs in our image data. It is recognised that the central area consisting of the optic nerve head will be fairly accurate, yet towards the edges of the SLO, the deformation is more noticable. This is influenced by the curvature of the back of the eye. Whilst the fundus image is simply a photograph, the SLO is an averaged image from slices taken in the Z-axis, and so there can be some differences. For the 16 windows used to break up our image, we limit the 4 central windows to a translation radius of 3 pixels and we limit the 12 outer windows to a translation radius of 5 pixels. This allows enough freedom to correct subtle misalignments without the windows shifting too far from the initial position, which prevents windows from becoming misplaced (e.g. if two windows shifted past each other and swapped position). As the final stage to our non-rigid registration we apply a thin-plate spline warp as proposed by Bookstein [10]. Thin-plate splines allow for an image to be deformed by 'bending' an image, much as if one was to bend a thin sheet of metal. The algorithm requires initialization using landmark control points, for which we use the initial centre-points of each window used in LWMI. The deformation for each point is the centre-point of each window after performing LWMI. The displacement between these points is then modelled by the thin-plate splines to determine how the image should be bent. This gives the final deformed image that is then positioned onto the reference image.

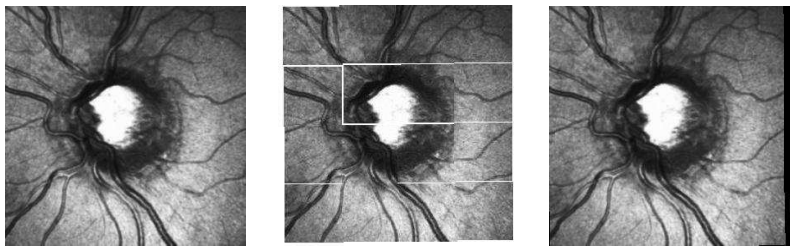

Figure 3. Left-to-right: Original template. Individually registered windows using LWMI. Result template.

4 Testing and Results

For our testing, we have 135 image pairs that are to be registered correctly, consisting of colour fundus photographs and scanning laser ophthalmoscope (SLO) images. For each image pair, we shall perform FNMI to find a rigid registration, and then perform LWMI to extend this to a non-rigid registration. Our implementation is written in MATLAB using a standard desktop PC with a 3.4 GHz CPU and 3GB RAM. To evaluate our results, we compare the Normalized Mutual Information scores obtained from rigid and non-rigid registration.

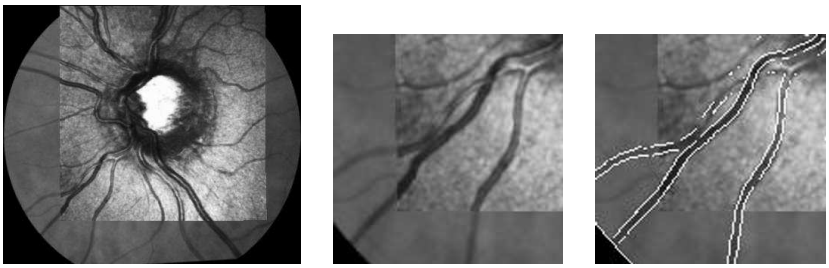

Figure 4. Left-to-right: Non-Rigid Registration using FNMI with LWMI. Corrected close-up from Fig. 2.

Figure 4 shows the correction to registration that non-rigid registration can offer. In this example we manage to improve the correspondence between the blood vessels in the bottom-left of the image whilst preserving good registration throughout the rest of our image. To assess the improvement of this approach compared to rigid registration, we compare the Normalized Mutual Information score for the rigid registrations (as given by FNMI) and for the non-rigid registrations (as given by FNMI with LWMI). We found that 99 of the 135 non-rigid registrations (73.3%) gave a greater Normalized Mutual Information score compared to the rigid registration, showing that there is a stronger correspondence between the matching images.

In the cases where a lower NMI score is given using non-rigid registration, we observe that while incorrect regions are corrected for, other parts of the image that were previously aligned can be affected by the deformation warp and become misaligned. Also, individual windows that contain less significant detail may give a poor registration result in LWMI that can affect the overall quality of the non-rigid deformation. Figure 5 shows a case where non-rigid registration achieves a lower NMI score. It can be observed that in the rigid registration that the top-left and bottom-centre of the registered region appear in good alignment. However, the top-centre, bottom-left and the right-hand side of the registered region all show signs of misalignment. The non-rigid registration improves the poor regions from the rigid registration however it fails to preserve the already-aligned regions. The NMI score for the rigid registration is 1.0498, compared to 1.0478 given by the non-rigid registration. This highlights the difficultly of quantifying the result by NMI score, since both images are fairly accurate but both suffer from different alignment errors. This would suggest that visual inspection may offer a better assessment of success.

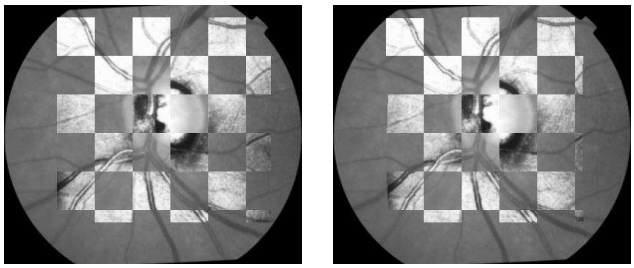

Figure 5. Rigid vs. Non-rigid registration where non-rigid gives a lower NMI score

In terms of computation time, to find the intial rigid registration using FNMI method takes on average 223.2 seconds. From here, the non-rigid registration can be found using LWMI in 16.4 seconds on average. Whilst the FNMI method can be quite time-consuming, it is important that our initial registration is accurate else the non-rigid registration will fail also. Using FNMI with a 3-stage pyramid, the coarse level of the pyramid takes on average approximately 40 seconds, which we considered using for our initial point for non-rigid registration. However, we found that the windows in the LWMI required a much larger translation shift which affected the performance of the thin-plate spline.

Figure 6 shows example cases between rigid and non-rigid registration. From visual inspection, we found that non-rigid registration gave good results in refining the initial registration. In each of these cases there are misalignments present in the rigid registrations that are corrected by non-rigid registration, tending to be most noticable towards the lower area

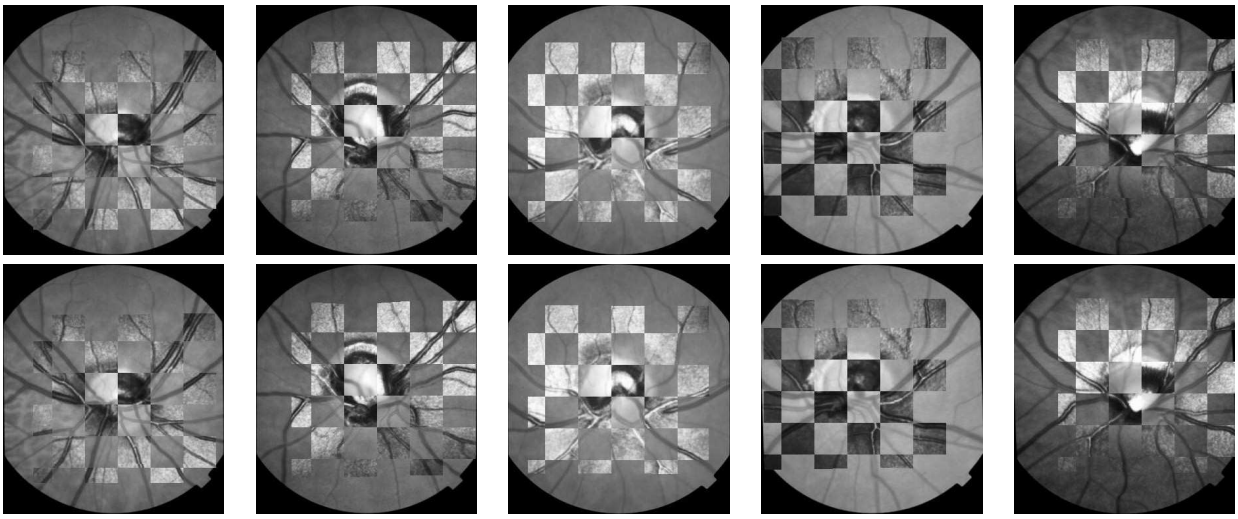

Figure 6. Top: Rigid registration results. Bottom: Non-rigid registration results.

of the registered region. Since the difference between rigid and non-rigid registration are still quite minimal, grading the images based on registration quality like in [1] would prove difficult as there is little noticable difference on first inspection. We found that for the 99 images that improve NMI, the actual registration accuracy is improved, which can be recognised by improved vessel alignment. In most other cases, we found that whilst parts of the registration were improved, other areas were weaker, and so it is difficult to quantify whether this is an improved registration (as shown in Figure 5). However, there are no cases where the non-rigid registration is significantly worse than the original rigid registration.

5 Discussion

We have proposed automated non-rigid registration of retinal images using Local Window Mutual Information. This method aims to improve local registration and then uses this to deform the floating image by using thin-plate spline warping. Our approach offers a fast solution for non-rigid registration in retinal images to correct any subtle misalignments that exist in the rigid registration. Currently we use Normalized Mutual Information to register our windows locally. Though NMI may fail for larger registration problems (such as finding the initial rigid registration), in cases such as this where the subimage is small and there is a limited translation space, the measure can provide a satisfactory result. Certainly in the interest of runtime, NMI can provide a fast solution which makes this an ideal similarity measure. Further work will investigate the possibility of improved MI-based measures, along with alternative deformation marker schemes, that aim to preserve accurate alignments obtained from rigid registration.

References

1. P. A. Legg, P. L. Rosin, D. Marshall et al. "Incorporating neighbourhood feature derivatives with mutual information to improve accuracy of multi-modal image registration." In *Medical Imaging Understanding and Analysis*, pp. 39–43. 2008.
2. B. Fang, X. You & Y. Y. Tang. "A novel fusing algorithm for retinal fundus images." In *Computational Intelligence and Security*. 2005.
3. P. A. Viola & W. M. Wells. "Alignment by maximization of mutual information." In *ICCV*, pp. 16–23. 1995.
4. A. Collignon, F. Maes, D. Delaere et al. "Automated multimodality medical image registration using information theory." In *Proc. 14th Int. Conf. Information Processing in Medical Imaging*, volume 3, pp. 263–274. June 1995.
5. C. Studholme, D. L. G. Hill & D. J. Hawkes. "An overlap invariant entropy measure of 3d medical image alignment." *Pattern Recognition* **32(1)**, pp. 71–86, 1999.
6. D. Rueckert, L. I. Sonoda, C. Hayes et al. "Non-rigid registration using free-form deformations: Application to breast MR images." *IEEE Trans. Med. Imaging* **18(8)**, pp. 712–721, 1999.
7. K. Rohr, M. Fornefett & H. S. Stiehl. "Approximating thin-plate splines for elastic registration: Integration of landmark errors and orientation attributes." In *Proc. of IPMI, volume 1613 of LNCS*, pp. 252–265. Springer, 1999.
8. L. Kubecka & J. Jan. "Registration of bimodal retinal images - improving modifications." *IEEE Int. Conf. on Engineering in Medicine and Biology* **1**, pp. 1695–1698, Sept. 2004.
9. J. C. Lagarias, J. A. Reeds, M. H. Wright et al. "Convergence properties of the Nelder-Mead simplex method in low dimensions." *SIAM Journal of Optimization* **9(1)**, pp. 112–147, 1998.
10. F. L. Bookstein. "Principal warps: Thin-plate splines and the decomposition of deformations." *IEEE Trans. Pattern Anal. Mach. Intell.* **11(6)**, pp. 567–585, 1989.